

Supplemental information

**The RNA helicase DHX16 recognizes specific
viral RNA to trigger RIG-I-dependent
innate antiviral immunity**

Adam Hage, Preeti Bharaj, Sarah van Tol, Maria I. Giraldo, Maria Gonzalez-Orozco, Karl M. Valerdi, Abbey N. Warren, Leopoldo Aguilera-Aguirre, Xuping Xie, Steven G. Widen, Hong M. Moulton, Benhur Lee, Jeffrey R. Johnson, Nevan J. Krogan, Adolfo García-Sastre, Pei-Yong Shi, Alexander N. Freiberg, and Ricardo Rajsbaum

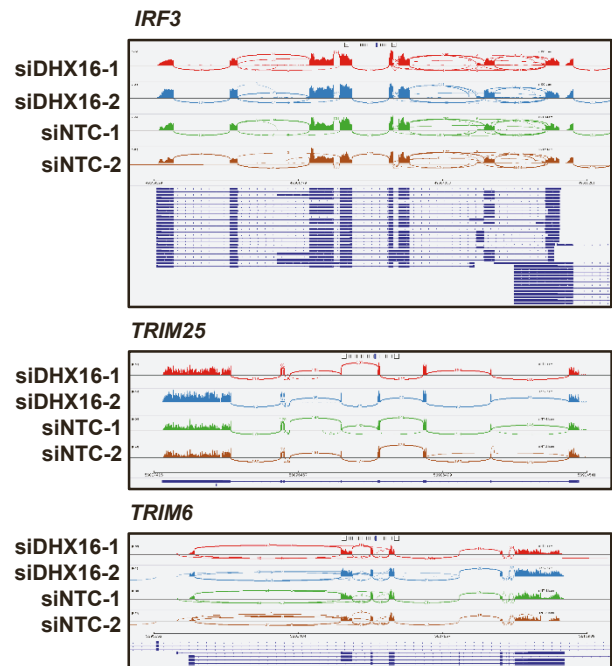
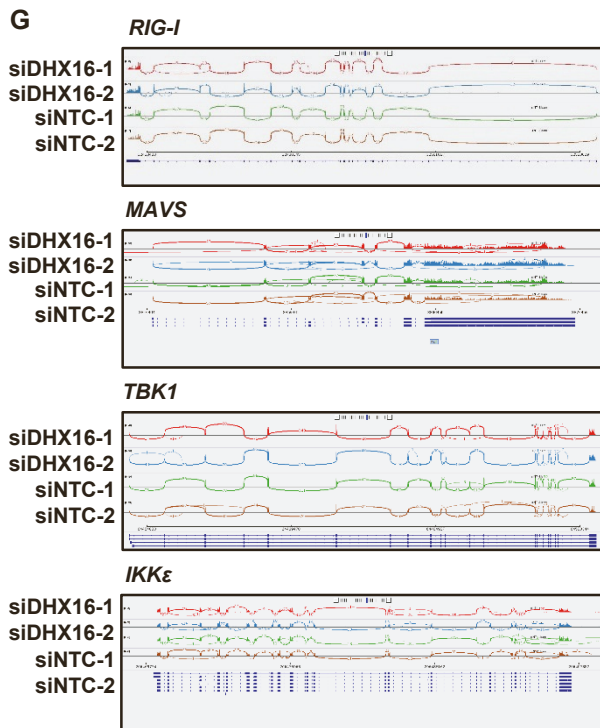
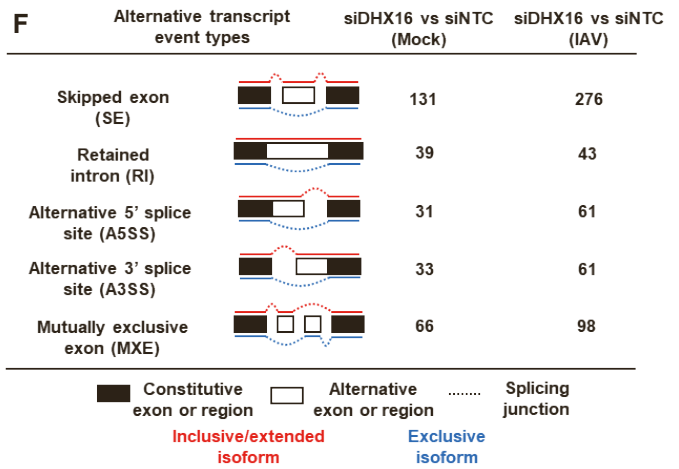
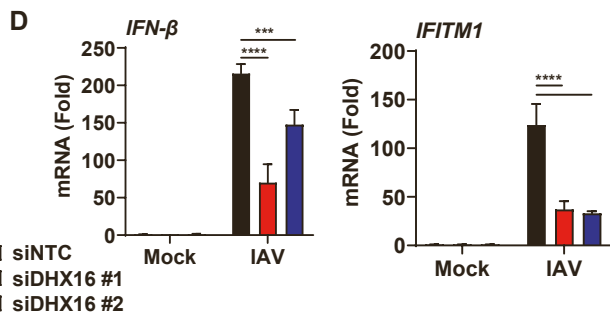
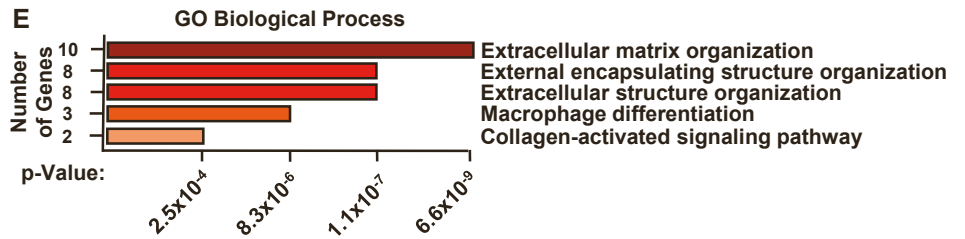
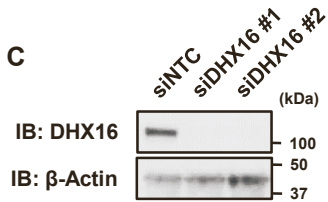
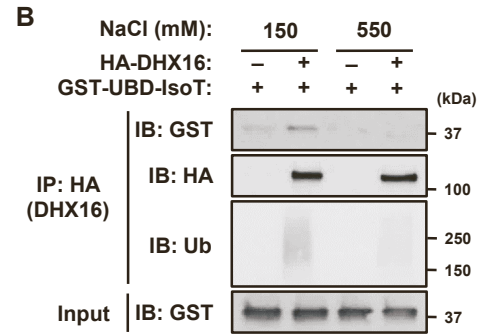
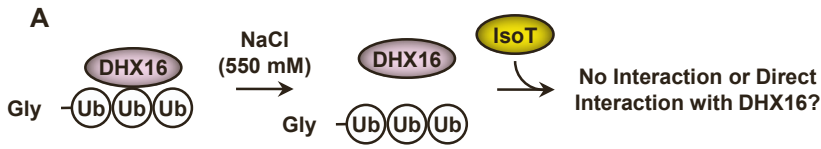


Figure S1. DHX16 knockdown does not alter splicing of IFN-I pathway genes. Related to Figures 1 and 2. (A) Representation of the denaturing Co-IP assay used to determine if IsoT interacts with DHX16 directly or indirectly via unanchored Ub. (B) GST-UBD-IsoT interacts with DHX16 *in vitro* via unanchored Ub after normal ionic strength (150 mM NaCl), but not high ionic strength (550 mM NaCl), RIPA washes (denaturing Co-IP). (C) Individual siRNA silencing efficiency of DHX16 protein expression (immunoblot). (D) *IFN- β* and *IFITM1* expression from siNTC or individual siDHX16 treated A549s stimulated with IAV for 24 hrs (PR8 MOI=0.1) (qRT-PCR). (E) Enriched GO terms and pathways (Enrichr) of upregulated transcripts identified in the NGS heat map. (F) Number of alternative exons between siNTC and siDHX16 treated mock or IAV-infected A549s. (G) RNA-seq reads of human *RIG-I*, *MAVS*, *TBK1*, *IKK ϵ* , *IRF3*, *TRIM25*, and *TRIM6* genes. Data are expressed as means (n=3) SD ***p < 0.001; ****p < 0.0001 (Two-way ANOVA with Dunnett's multiple comparisons). Data are representative of 2-3 independent experiments.

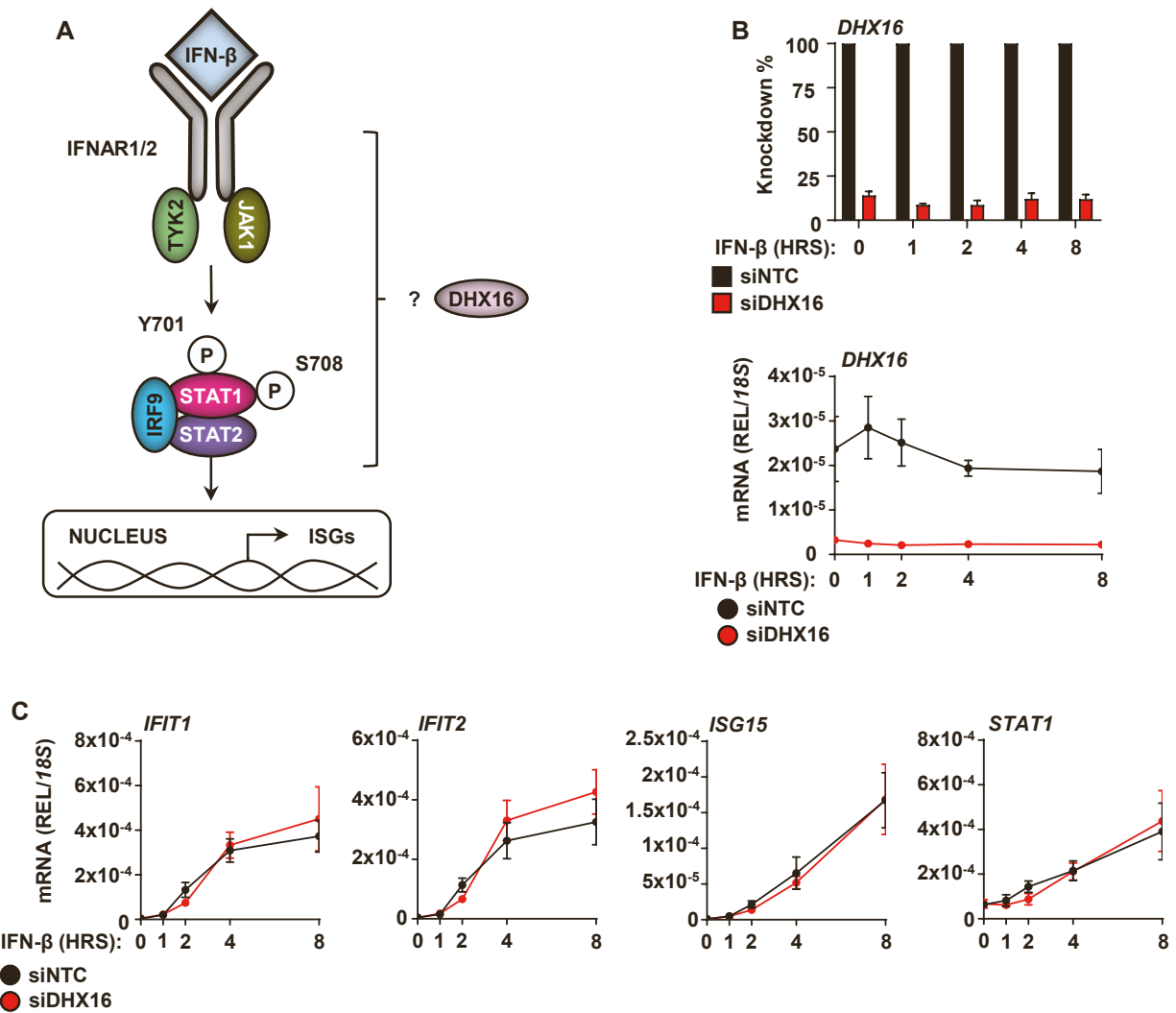


Figure S2. DHX16 is not an IFN-stimulated gene. Related to Figure 3. (A) Diagram of IFN-signaling pathway. (B) *DDX16* expression from siNTC or siDDX16 treated A549s stimulated with IFN- β (1000 IU/mL) (qRT-PCR). (C) ISG expression from siNTC or siDDX16 treated A549s stimulated with IFN- β (1000 IU/mL) (qRT-PCR). Data are expressed as means (n=3) \pm SD (Student's t-test). Data are representative of 2-3 independent experiments.

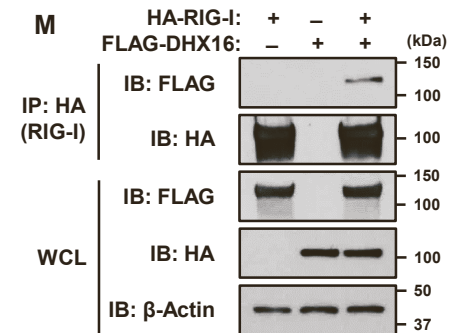
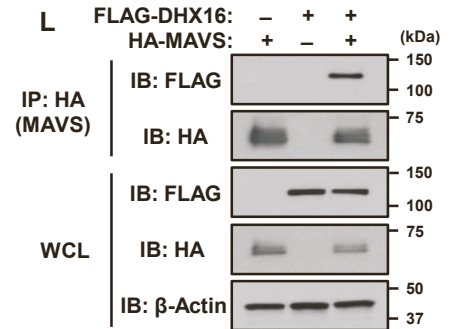
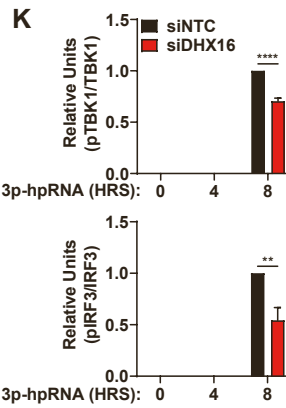
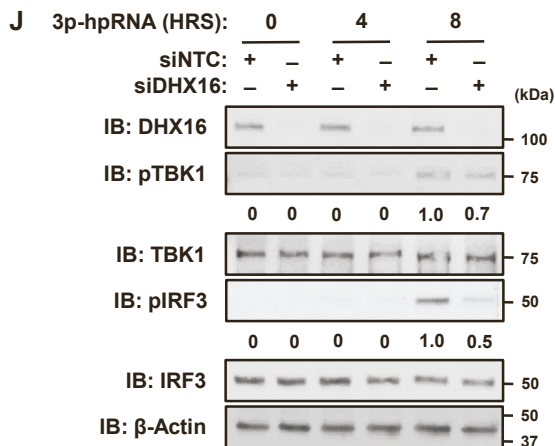
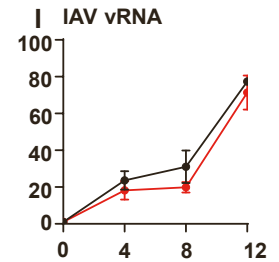
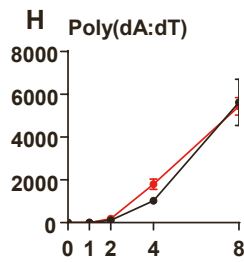
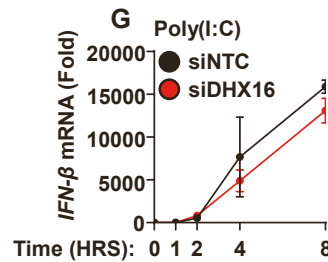
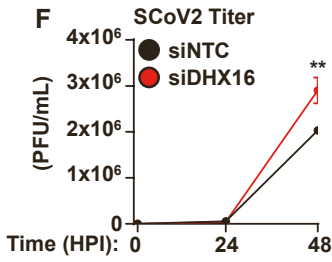
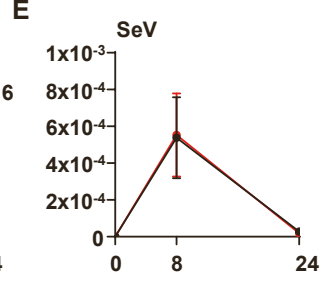
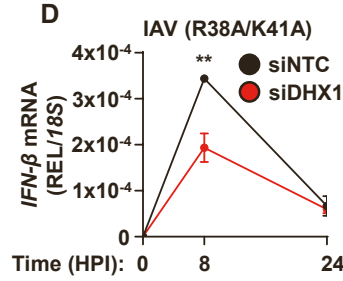
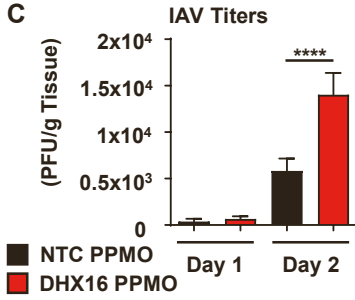
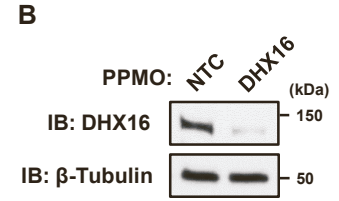
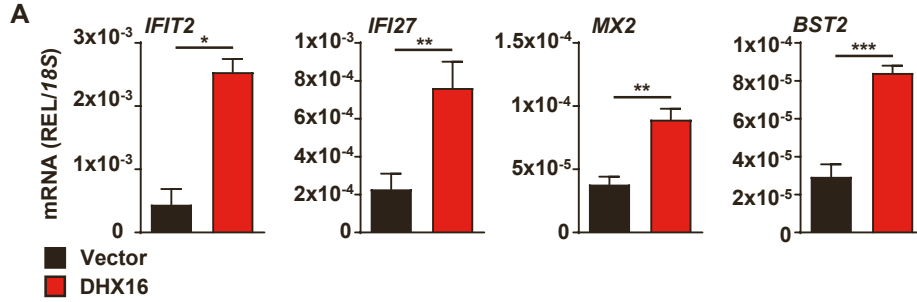


Figure S3. DHX16 promotes the IFN-I production pathway. Related to Figure 3 and 4. (A) *IFIT2*, *IFI27*, *Mx2*, and *BST2* expression from A549s transfected with DHX16 for 24 hrs (qRT-PCR). (B) Validation of PPMO-mediated silencing efficiency of DHX16 in MEFs (immunoblot). (C) Viral titers from NTC or DHX16 PPMO treated C57BL/6 mice infected with IAV (PR8 100 PFU) (n=3-4/group). (D and E) *IFN-β* expression from siNTC or siDHX16 treated A549s infected with IAV (PR8 R38A/K41A MOI=0.1) (D), or SeV (Cantell 100 HAU/mL) (E) (qRT-PCR). (F) Viral titers from siNTC or siDHX16 treated Calu-3s infected with SCoV2 (icSARS-CoV-2-mNG MOI=1). (G-I) *IFN-β* expression from siNTC or siDHX16 treated A549s transfected with Poly(I:C) HMW (10 μg/mL) (G), Poly(dA:dT) (10 μg/mL) (H), or IAV vRNA (100 ng/mL) (I) (qRT-PCR). (J) IFN-I production pathway activation from siNTC or siDHX16 treated A549s stimulated with 3p-hpRNA (100 ng/mL) (immunoblot). (K) Western blot quantification for pTBK1 and pIRF3 in (J) (densitometry). (L) Interaction between DHX16 and MAVS following co-expression in HEK293Ts (Co-IP). (M) Reciprocal interaction between DHX16 and RIG-I following co-expression in HEK293Ts (Co-IP). Data are expressed as means (n=3) SD *p < 0.05; **p < 0.01; ***p < 0.001; ****p < 0.0001 (Student's t-test or one-way ANOVA with Tukey's multiple comparisons). Data are representative of 2-3 independent experiments.

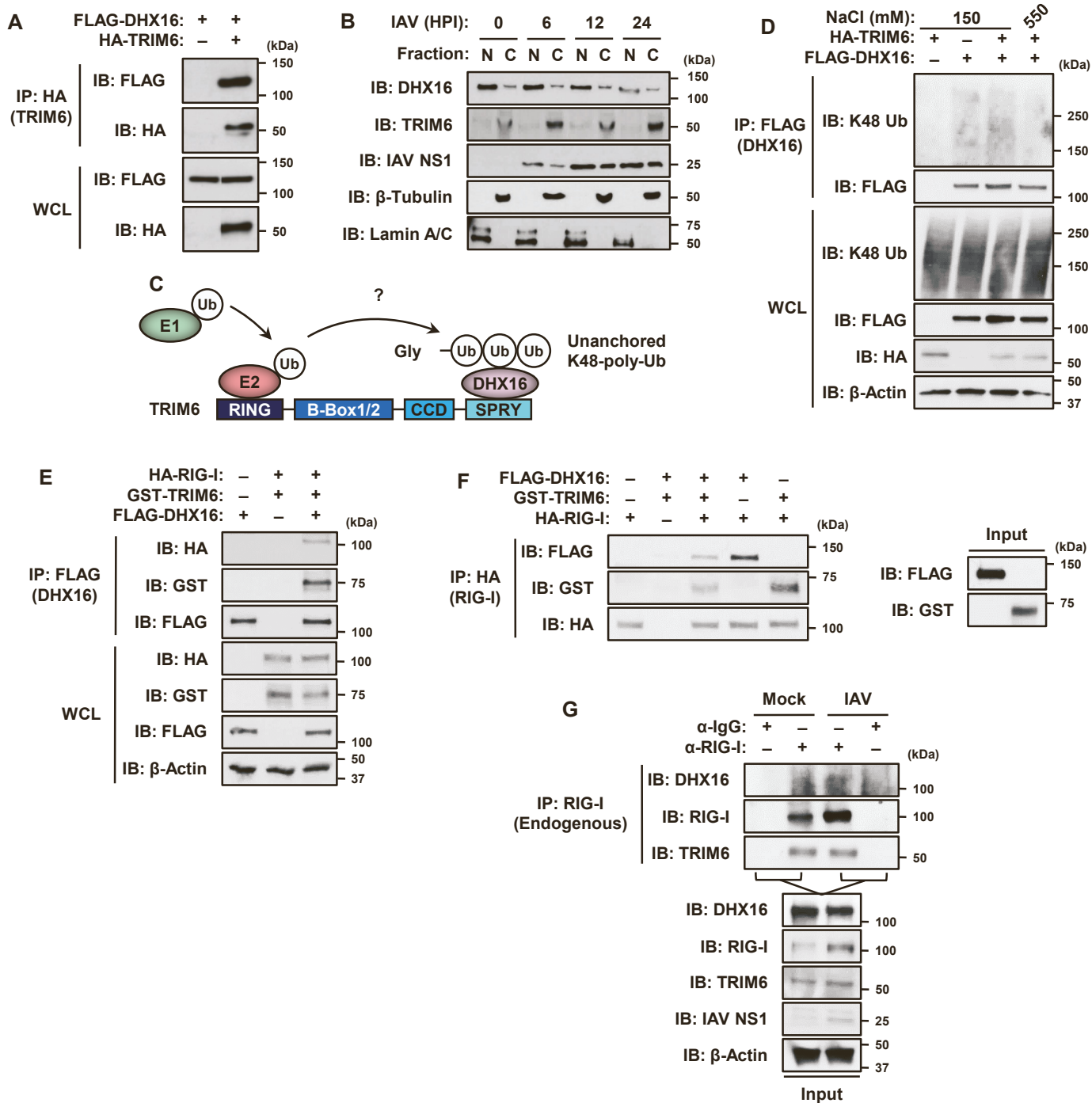


Figure S4. DHX16 interacts with TRIM6. Related to Figure 6. (A) Reciprocal interaction between DHX16 and TRIM6 following co-expression in HEK293Ts (Co-IP). (B) Nuclear and cytoplasmic distribution of DHX16 in mock and IAV infected A549s (PR8 MOI=1) (immunoblot). (C) Representation of RING and SPRY domain involvement in the TRIM6-mediated association of poly-Ub to targets. (D) Non-covalent interactions between DHX16 and K48-poly-Ub following co-expression with WT TRIM6 in low, but not high, salt washes in HEK293Ts (denaturing Co-IP). (E) Interaction between DHX16, RIG-I, and TRIM6 following co-expression in HEK293Ts (Co-IP). (F) Interaction between purified DHX16, RIG-I, and TRIM6 protein *in vitro* (Co-IP). (G) Interaction between endogenous DHX16, RIG-I, and TRIM6 in A549s infected with IAV for 24 hrs (PR8 MOI=1) (Co-IP). Data are representative of 2-3 independent experiments.

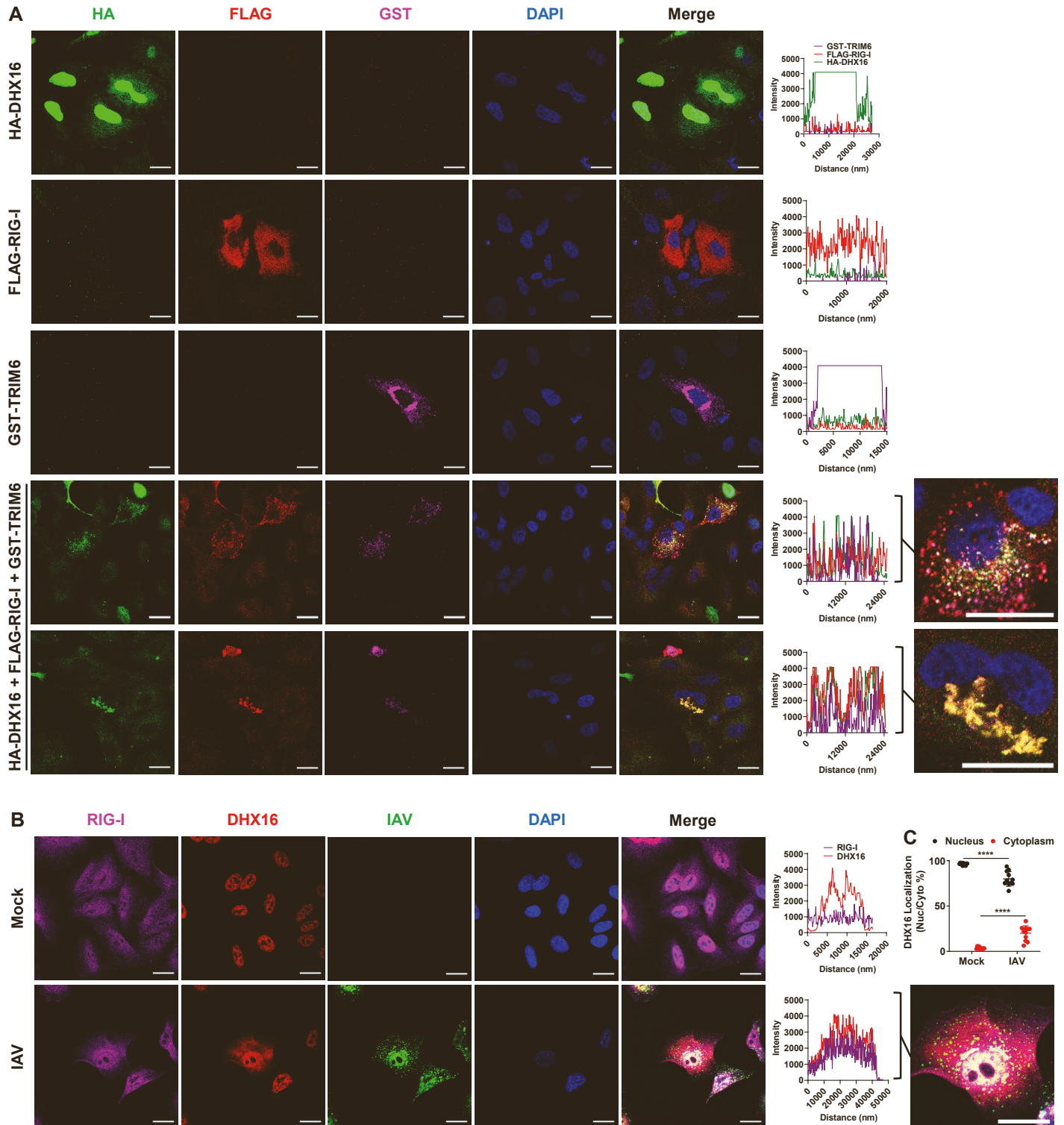


Figure S5. DHX16 interacts with RIG-I and TRIM6 in the cytoplasm. Related to Figure 6. (A) Co-localization between DHX16, RIG-I, and TRIM6 following co-expression in A549s. **(B)** Co-localization between DHX16 and RIG-I following IAV infection for 24 hrs in A549s (PR8 MOI=1). Scale bar=20 μ m (confocal microscopy). **(C)** Nuclear/cytoplasmic distribution of DHX16 following IAV infection for 24 hrs in A549s (PR8 MOI=1) (n=11). Data are expressed as means \pm SD ****p < 0.0001 (Two-way ANOVA with Tukey's multiple comparisons). Data are representative of 2-3 independent experiments.

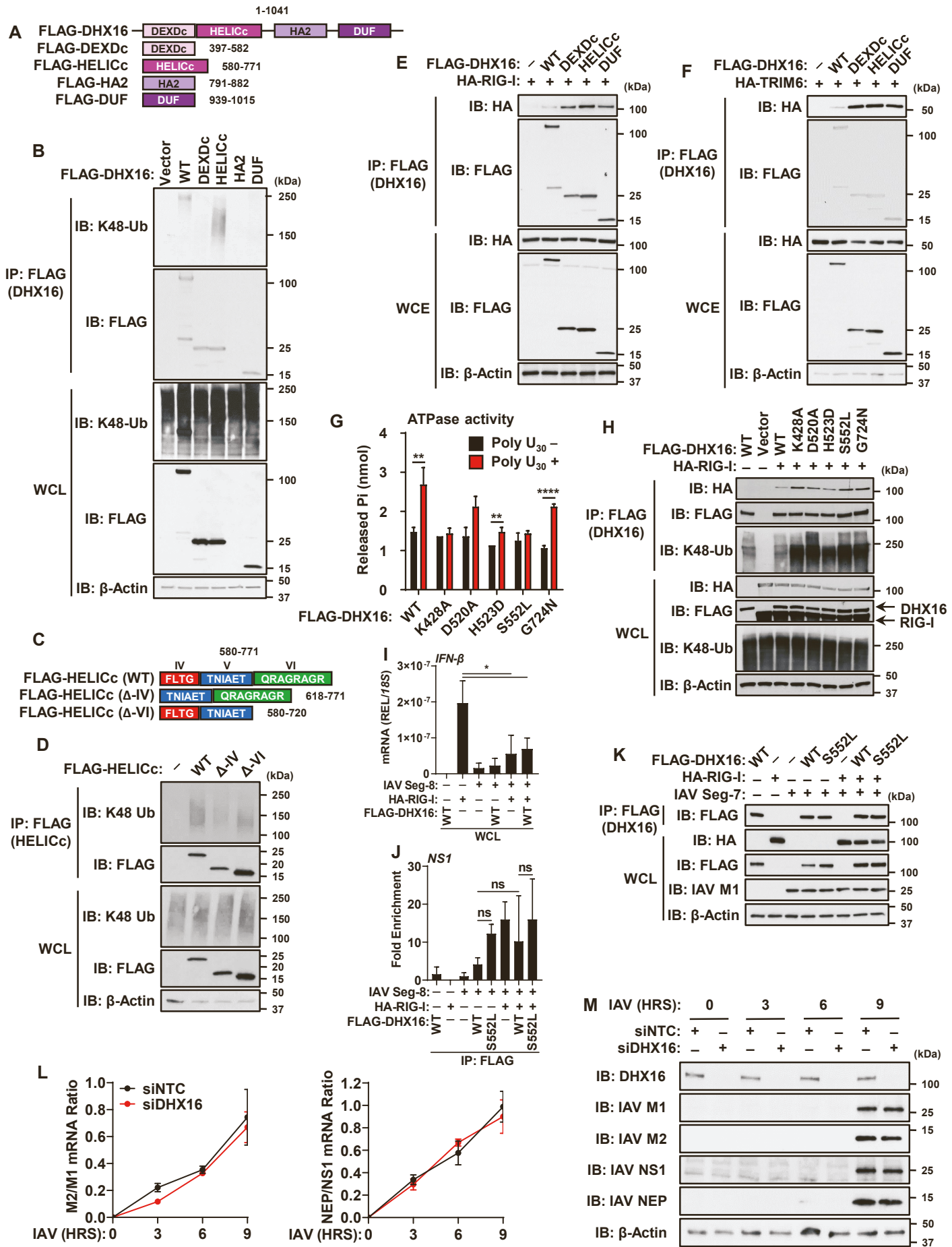


Figure S6. DHX16 knockdown does not alter splicing of IAV genes. Related to Figure 7. (A) Diagram of DHX16 domains mutants used. (B) Interactions between DHX16 (WT and domain mutants) and K48-poly-Ub following co-expression in HEK293Ts (Co-IP). (C) Diagram of DHX16-HELICc motif mutants used. (D) Interactions between DHX16-HELICc (WT and motif mutants) and K48-poly-Ub following co-expression in HEK293Ts (Co-IP). (E and F) Interactions between DHX16 (WT and domain mutants) and RIG-I (E) or TRIM6 (F) following co-expression in HEK293Ts (Co-IP). (G) ATPase activity of DHX16 (WT or mutants) in an *in vitro* ATPase assay. (H) Interactions between DHX16 (WT and mutants) and RIG-I following co-expression in HEK293Ts (Co-IP). (I) Input *IFN-β* expression from IAV segment 8 RNA-IP (qRT-PCR). (J) Interaction between DHX16 (WT or S552L) and segment 8 of IAV in the presence or absence of RIG-I (fold enrichment over segment 8 alone) (RNA-IP). (K) Input protein expression from RNA-IP using IAV segments (immunoblot). (L) *M2/M1* and *NEP/NS1* expression from siNTC or siDHX16 treated A549s infected with IAV (PR8 MOI=1) (qRT-PCR). (M) Expression of IAV proteins from siNTC or siDHX16 treated A549s infected with IAV (PR8 MOI=1) (immunoblot). Data are expressed as means (n=3) SD *p < 0.05; **p < 0.01; ****p < 0.0001 (Student's t-test or one-way ANOVA with Tukey's multiple comparisons). Data are representative of 2-3 independent experiments.

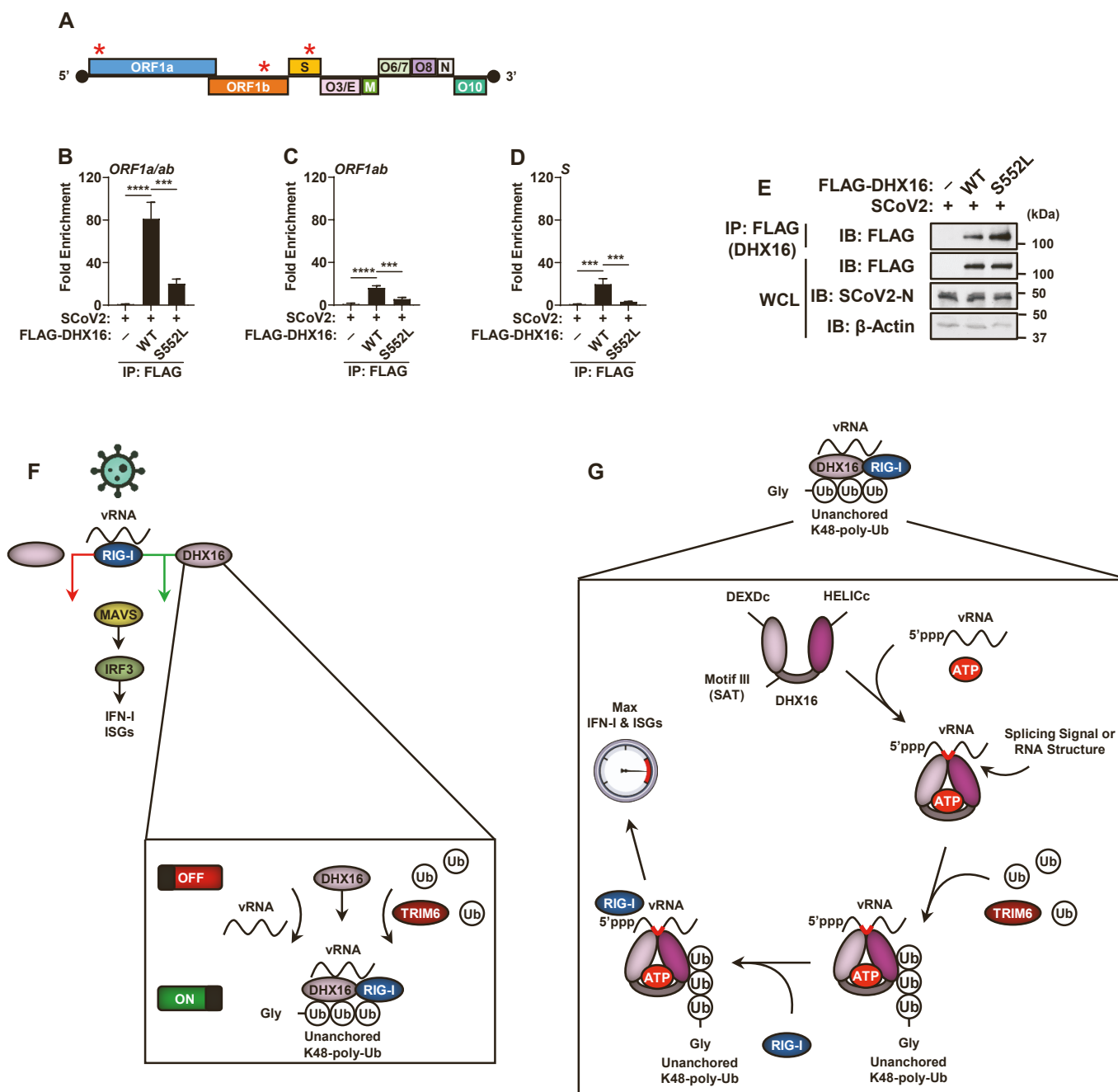


Figure S7. DHX16 enhances IFN-I production in response to virus infection. Related to Figure 7. (A) Diagram of SCoV2 genome. Stars indicate amplification regions of qRT-PCR primers used. (B-D) Interaction between DHX16 (WT or S552L) and SCoV2 vRNAs from HEK293T-hACE2s infected for 24 hrs (USA-WA1/2020 MOI=0.1) (fold enrichment over SCoV2 alone) (RNA-IP). (E) Input protein expression from RNA-IP using SCoV2 (immunoblot). (F and G) Model of DHX16-dependant enhancement of antiviral innate immunity. (F) DHX16 enhances RIG-I-mediated IFN-I production in response to virus infection. Activation of DHX16 requires recognition of vRNA and interactions with unanchored K48-poly-Ub chains synthesized by TRIM6. These interactions promote the recruitment of RIG-I. (G) Sensing of vRNAs by DHX16 requires specific PAMPs (splicing signals in IAV and potentially RNA structures or Poly U sequences for other viruses). This recognition requires an intact motif III (SAT) which utilizes the binding energy of ATP to alter the conformation of the helicase domain into a high-affinity RNA clamp. Upon engagement with an RNA substrate, K48-poly-Ub chains synthesized by TRIM6 associate with DHX16's HELICc domain. The presence of these unanchored Ub chains facilitate interactions with RIG-I, which is required for the DHX16-dependent enhancement of downstream IFN-I signaling and optimal antiviral innate immunity. Data are expressed as means (n=3) SD ***p < 0.01; ****p < 0.0001 (One-way ANOVA with Tukey's multiple comparisons). Data are representative of 2-3 independent experiments.

SUPPLEMENTAL TABLES

Table S1: Primer sequences to generate mutations and fusion constructs for DHX16, related to STAR Methods.

CONSTRUCT	FORWARD	REVERSE
Oligonucleotides for cloning constructs		
HA-DHX16	5'- ATAATAGAATTCATG GCGACGCCGGCGG GTCTGGAGCGCTGG GTTTCAGGACGAGCT GCACTCGGTGTTG- 3'	5'- TAATATCTCGAGTT AGTAATCTGGAAC ATCGTATGGGTAC ATTGCTGCTGCC CTAGCTCTTCTCG TGTTTTG-3'
FLAG-DHX16 (K428A)	5'- AGACAGGCTCAGGG GCGACCACCCAGAT -3'	5'- ATCTGGGTGGTCG CCCCTGAGCCTGT CT-3'
FLAG-DHX16 (D520A)	5'- CGTGGTGATGGTGG CAGAGGCACACGAA A-3'	5'- TTTCGTGTGCCTC TGCCACCATCACC ACG-3'
FLAG-DHX16 (H523D)	5'- TGGTGGATGAGGCA GATGAAAGGACCCT ACACACAGA-3'	5'- TCTGTGTGTAGGG TCCTTTCATCTGC CTCATCCACCA-3'
FLAG-DHX16 (S552L)	5'- TCAAGGTCCTGGTG GCTTTAGCCACAAT GGACACT-3'	5'- AGTGTCCATTGTG GCTAAAGCCACCA GGACCTTGA-3'
FLAG-DHX16 (G724N)	5'- ATTAGAATTCGTCTGA CTGGATCCGGTACC GAGGAGATCT-3'	5'- TAATGTATACAGG CGGAAGCACTTCC CTGCAGCCACCCG ACCTGCCCTGTTA GCTCGCTGAT-3'
FLAG-DHX16 (DEXDc)	5'- ATTAGCGATCGCCA TGAGCCTCCCGGTG TTC-3'	5'- TAATACGCGTGAA GATGTCCACAGGA AACCT-3'
FLAG-DHX16 (HELICc)	5'- ATTAGCGATCGCCA TGGACATCTTCTACA -3'	5'- TAATACGCGTCCC TAAGCTCTTGAGC AGCAACA-3'
FLAG-DHX16 (HA2)	5'- ATTAGCGATCGCCA TGCTGGCTTTGGAG CAGCTGTAT-3'	5'- TAATACGCGTTAG CAGAACCAGGTGG TCA-3'

FLAG-DHX16 (DUF)	5'- ATTAGCGATCGCCA TGGTACGCAAGGCC ATCACT-3'	5'- TAATACGCGTATA ATGGGGAGCCAC CTCCAGAA-3'
FLAG-DHX16 (HELICc Δ-IV)	5'- ATTAGCGATCGCCA TGCCCATTTATGCC AATCTGCCCTCT-3'	5'- TAATACGCGTCCC TAAGCTCTTGAGC AGCAACA-3'
FLAG-DHX16 (HELICc Δ-VI)	5'- ATTAGCGATCGCCA TGGACATCTTCTACA -3'	5'- TAATACGCGTGCT CTTCTGCTTACAG AACCT-3'

Table S2: Primer sequences to determine mRNA transcript levels, related to STAR Methods.

REAGENT or RESOURCE	FORWARD	REVERSE
Oligonucleotides for qRT-PCR		
<i>h18S rRNA</i>	5'- GTAACCCGTTGAAC CCCATT-3'	5'- CCATCCAATCGGT AGTAGCG-3'
<i>hDHX16</i>	5'- CCAACCTGCTCTCAA TCTCCA-3'	5'- ATCCCAACTCCTC CCTCTTT-3'
<i>hIFN-β</i>	5'- TCTGGCACAACAGG TAGTAGGC-3'	5'- GAGAAGCACAACA GGAGAGCAA-3'
<i>hIFIT1</i>	5'- CAAAGGGCAAACG AGGCAG-3'	5'- CCCAGGCATAGTT TCCCCAG-3'
<i>hIFITM1</i>	5'- TGACCATTGGATTC ATCCTG-3'	5'- TGCACAGTGGAGT GCAAAG-3'
<i>hIFIT2</i>	5'- ATGTGCAACCTACT GGCCTAT-3'	5'- TGAGAGTCGGCCC ATGTGATA-3'
<i>hIFI27</i>	5'- ACTGGGAGCAACTG GACTCT-3'	5'- TAGAACCTCGCAA TGACAGC-3'
<i>hMX2</i>	5'- AGGTTCCAGACCTG ACCATC-3'	5'- GTCTGCTGCCTCT GGATGTA-3'
<i>hBST2</i>	5'- GAAAGTGGAGGAGC TTGAGG-3'	5'- ACTTCTTGCCGC GATTCTC-3'
<i>hISG15</i>	5'- TCCTGGTGAGGAAT ACAAGGG-3'	5'- GTCAGCCAGAACA GGTCGTC-3'

<i>hSTAT1</i>	5'- ACAGCAGAGCGCCT GTATTG-3'	5'- CAGCTGATCCAAG CAAGCAT-3'
<i>mβ-Actin</i>	5'- CGGTTCCGATGCC TGAGGCTCTT-3'	5'- CGTCACACTTCAT GATGGAATTGA-3'
<i>mIFN-β</i>	5'- CAGCTCCAAGAAAG GACGAAC-3'	5'- GGCAGTGTAAC TTCTGCAT-3'
<i>mIFITM1</i>	OriGene Cat #MP206689	OriGene Cat #MP206689
<i>IAV NP</i>	5'- GCCTGCCTGCCTGT GTGTATGGAT-3'	5'- GGCATGCCATCCA CACCAGTTGAC-3'
<i>IAV M1</i>	5'- AGATGAGTCTTCTAA CCGAGTCG-3'	5'- TGCAAAAACATCT TCAAGTCTCT-3'
<i>IAV M2</i>	5'- CCGAGGTCGAAACG CCTATCAG-3'	5'- GCAATAGTGAGAG GATCACTTGAAC-3'
<i>IAV NS1</i>	5'- GATCCAAACACTGT GTCAAGCTTTC-3'	5'- ATCCGCTCCACTA TCTGCTT-3'
<i>IAV NEP</i>	5'- GGGTGACAAAGACA TAATGG-3'	5'- TCTCCCATTCTCAT TACTGC-3'
<i>SCoV2 ORF1a/ab</i>	5'- AGTTACGGCGCCGA TCTAAAGTCAT-3'	5'- TAGCCATCAGGGC CACAGAAGTT-3'
<i>SCoV2 ORF1ab</i>	5'- TACGTGCATGGATT GGCTTCGAT-3'	5'- GTTTAAATTGATCT CCAGGCGGTGGT- 3'
<i>SCoV2 S</i>	5'- GCCTTACTGTTTTGC CACCT-3'	5'- TGATTGTACCCGC TAACAGTGC-3'